Contents lists available at ScienceDirect

Clinical and Translational Radiation Oncology

Original Research Article

4D-MRI driven MR-guided online adaptive radiotherapy for abdominal stereotactic body radiation therapy on a high field MR-Linac: Implementation and initial clinical experience

Eric S. Paulson [a,b,c,*], Ergun Ahunbay [a], Xinfeng Chen [a], Nikolai J. Mickevicius [a], Guang-Pei Chen [a], Christopher Schultz [a], Beth Erickson [a], Michael Straza [a], William A. Hall [a], X. Allen Li [a]

[a] Department of Radiation Oncology, Medical College of Wisconsin, Milwaukee, WI, United States
[b] Department of Radiology, Medical College of Wisconsin, Milwaukee, WI, United States
[c] Department of Biophysics, Medical College of Wisconsin, Milwaukee, WI, United States

ABSTRACT

Background and purpose: In this report, we describe our implementation and initial clinical experience using 4D-MRI driven MR-guided online adaptive radiotherapy (MRgOART) for abdominal stereotactic body radiotherapy (SBRT) on the Elekta Unity MR-Linac.
Materials and methods: Eleven patients with abdominal malignancies were treated with free-breathing SBRT in three to five fractions on a 1.5 T MR-Linac. Online adaptive plans were generated using Adapt-To-Position (ATP) or Adapt-To-Shape (ATS) workflows based on motion averaged or mid-position images derived from a pre-beam 4D-MRI. A high performance server positioned on the local MR-Linac machine network was utilized for 4D-MR image reconstruction. A parallel contour editing approach was employed in the ATS workflow. Intravoxel incoherent motion (IVIM) and T2 mapping sequences were acquired during adaptive planning in both ATP and ATS workflows for treatment response monitoring. Adaptive plans were delivered under real-time cine image motion monitoring.
Results: The shortest 4D-MRI time-to-image was the motion averaged image, followed by mid position and respiratory binned images. In this cohort of patients, 50% of treatments utilized the ATS workflow; the remaining treatments utilized the ATP workflow. Mid-position images were utilized as daily planning images for two of the eleven patients. The mean daily adaptive plan secondary dose calculation and ArcCheck 3D Gamma passing rates were 97.5% (92.1–100.0%) and 99.3% (96.2–100.0%), respectively. The median overall treatment times for abdominal SBRT was 46 and 62 min for ATP and ATS workflows, respectively.
Conclusion: We have successfully implemented and utilized a 4D-MRI driven MRgOART process with ATP and ATS workflows for free-breathing abdominal SBRT on a 1.5 T Elekta Unity MR-Linac.

1. Introduction

MR-guided online adaptive radiotherapy (MRgOART) offers unique potential to safely escalate radiotherapy doses to mobile tumors in the abdomen [1]. One such system capable of performing these treatments is the Elekta Unity MR-Linac, which combines a Philips 1.5 T MRI with a flattening filter free (FFF) Elekta 7MV linear accelerator [2]. In addition to providing high soft tissue contrast for anatomical definition and enabling intrafraction motion monitoring, the Unity system also permits acquisition of quantitative MR images for treatment response monitoring [3].

Unlike conventional linacs, the couch on the Unity system is restricted to motion along the superior-inferior direction and is not allowed to move once the patient is positioned. Therefore, every treatment fraction requires an adaptive plan. Once a daily MR image of the patient is obtained, online adaptive plans can be generated using one of two workflows: i) Adapt-To-Position (ATP) in which the reference plan is reoptimized with an isocenter shift determined from co-registration of the daily and reference images, or ii) Adapt-To-Shape (ATS) in which a new plan is generated based on the anatomy of the day [4]. The adaptive plan from

* Corresponding author at: Medical College of Wisconsin, 9200 Wisconsin Avenue, Milwaukee, WI 53226, United States.
E-mail address: epaulson@mcw.edu (E.S. Paulson).

either ATP or ATS can then be delivered under continuous real-time MR imaging of the target.

At the time of this writing, only free-breathing treatment deliveries are clinically supported on the Unity system; fully automated motion management capabilities (e.g., respiratory gating, breath-hold gating, trailing, tracking, or real-time plan adaptation) are not yet clinically available. With the small margins and high doses employed in stereotactic body radiotherapy (SBRT), knowledge of target and organs at risk (OAR) motion trajectories during free-breathing is critical. For MRgOART, a natural method of providing this information is four-dimensional (4D) MRI [5]. In addition, 4D-MRI eliminates systematic offsets between planned and delivered anatomies arising from breath hold or triggered image acquisitions and free-breathing treatment deliveries.

The purpose of this report is to describe our implementation and initial clinical experience using 4D-MRI driven MRgOART for abdominal SBRT on the Elekta Unity MR-Linac. To our knowledge, this is the first report using 4D-MRI in an online radiation therapy workflow.

2. Materials and methods

Eleven patients with abdominal malignancies were treated with free-breathing SBRT in three-to-five fractions on a 1.5 T Unity MR-Linac (Elekta, Stockholm, Sweden) over a six-month span from January through June 2019. Patient characteristics are provided in Supplementary Table S1. Patients signed informed consent for advanced MR imaging under guidelines established by the local Institutional Review Board at our Institution.

2.1. Patient simulation

Patients were positioned using one of three upper extremity positions: arms above head, one arm down, or both arms down. A foam template of the bore and array coils was used to verify compatibility of the patient setup with the MR-Linac. 4D-CT and dual-energy contrast-enhanced CT images were acquired on a Siemens Drive CT simulator (Siemens Healthcare, Erlangen, Germany). A time averaged mid-position (MidP) image [6] was derived from the 4D-CT in MIM 6.8.6 (MIM Software, Cleveland, OH). The MidP CT image was used as the reference studyset for reference plan generation. Respiratory-correlated 4D [5], fat-suppressed T2, and multiphase dynamic contrast T1w MRI images were acquired on a Siemens 3T Verio MR Simulator with patients setup in treatment position [7]. Respiratory-correlated 4D MR images were acquired using a 3D golden angle radial stack of stars (GAR SoS) sequence of our design and reconstructed using XD-GRASP [5,8,9]. Contrast-enhanced CT and MR simulation images were rigidly co-registered to MidP CT images in MIM. Internal target volumes (ITV) were determined from 4D-CT or 4D-MR scans of the patients. A 3–5 mm expansion of the ITV formed the planning target volume (PTV).

2.2. Reference plan generation

Reference plans were generated in Monaco 5.4 (Elekta, Stockholm, Sweden). Dose was calculated with GPUMCD [10] incorporating a transverse 1.5 T magnetic field [11]. The dose engine was verified recently with measurements [12]. An arrangement of ten to eighteen beams was used for reference plans with 3 mm grid size and 1% statistical uncertainty per plan. The initial fluence optimization was performed using constrained multicriterial optimization. Segment optimization was performed using Pareto optimization without multicriteria optimization. The Unity online adaptive workflow utilizes bulk density overrides for dose calculation on daily MR images. To determine the optimal patient density for override, the reference plan was recalculated with air, bone, and lung densities forced and the patient density was adjusted iteratively until the closest dose distribution to the reference plan was obtained.

For patients meeting selection criteria for ATS treatments (see Table 1), the reference plan was also templated and reoptimized on MR images of the patients with updated contours. This process simulated the ATS workflow and confirmed that the IMRT constraints in the reference plan were sufficiently robust for target and OAR deformations and changes in relative position of both.

2.3. Online workflow

A flow diagram of the MRgOART workflow for abdominal SBRT is shown in Fig. 1. Each MR-gOART fraction can be divided into three phases: pre-beam, beam-on, and post-beam. Imaging, treatment planning, and radiation delivery can occur individually or simultaneously in each of these phases. The MR-Linac team consisted of two radiation therapists, one medical physicist, and one radiation oncologist. Similar to other institutions utilizing MRgOART, checklists were developed and implemented to prevent inadvertent missing of critical workflow steps. The checklists are available for download as supplementary material.

2.3.1. Pre-beam 4D-MRI

The Philips 3D Vane sequence (a 3D GAR SoS sequence analogous to that used during MR Sim) was used for respiratory-correlated 4D-MRI acquisition. The optimal one of four image contrasts (T1-weighted, fat-suppressed T1-weighted, mixed T2/T1-weighted, and fat-suppressed mixed T2/T1-weighted) that maximized tumor visibility was selected by the treating physician in a separate pre-treatment imaging study. Basic sequence parameters included 1.6 mm in-plane resolution, 42 acquired partitions (84 slices after interpolation), 2.38 mm slices. Specific sequence details are provided in Supplementary Table S2. The number of partitions was chosen as a tradeoff between spatial coverage and maintaining respiratory navigator sampling at or above 5 Hz. Following acquisition, raw k-space data were transferred to a high-performance reconstruction computer (96 core Intel Xenon Platinum 2.7 GHz, 256 GB RAM) placed on the local MR-Linac machine network (see Fig. 2). Three sets of images were reconstructed from each 3D Vane acquisition using custom Matlab (The Mathworks, Natick, MA) software. First, a motion averaged image (MotAvg) was reconstructed from the full acquisition without rebinning. Second, an eight-frame respiratory binned time series was reconstructed using CG-SENSE [9,13]. Finally, a MidP image was generated from the reconstructed, binned 4D data. Each reconstructed series was corrected for gradient nonlinearities in 3D with ReconFrame (GyroTools LLC, Zurich, Switzerland) using the spherical harmonic coefficients from the Unity system. Following reconstruction, images were transferred to Monaco or MIM, depending on chosen workflow (see Fig. 2). Depending on the magnitude of respiratory displacement of the target and consistency of breathing, MotAvg (S/I respiratory displacements <0.8 cm or poor breathing consistency) or MidP images (S/I respiratory displacements >0.8 cm with good breathing consistency) were used for daily adaptation.

Table 1
Selection criteria for Adapt-To-Shape (ATS) workflow.

- Rotating or deforming structures in high dose region
- Potential for target motion changes
- Potential for moving air cavities
- Close proximity of deforming or rotating OARs in high dose regions
- Potential for radiological depth changes during treatment

	Pre-Beam			Beam-On	Post-Beam		
Imaging	4D-MRI Pre	qMRI (IVIM, CPMG, B0 Map)	4D-MRI Verify	Real-Time Cine Imaging	4D-MRI Post		
Planning		Contour Transfer and Parallel Editing	Adaptive Re-Planning			Reconstruct Dose	Accumulate Dose
Delivery				IMRT			

Fig. 1. MR-guided online adaptive workflow employed for abdominal SBRT Adapt-To-Shape (ATS) treatments on the Elekta Unity MR-Linac. Continuous acquisition of MR images is performed while the patient is on the treatment table (shaded boxes). For Adapt-To-Position (ATP) treatments, the contour transfer and parallel editing and 4D-MRI verification blocks are skipped in the workflow.
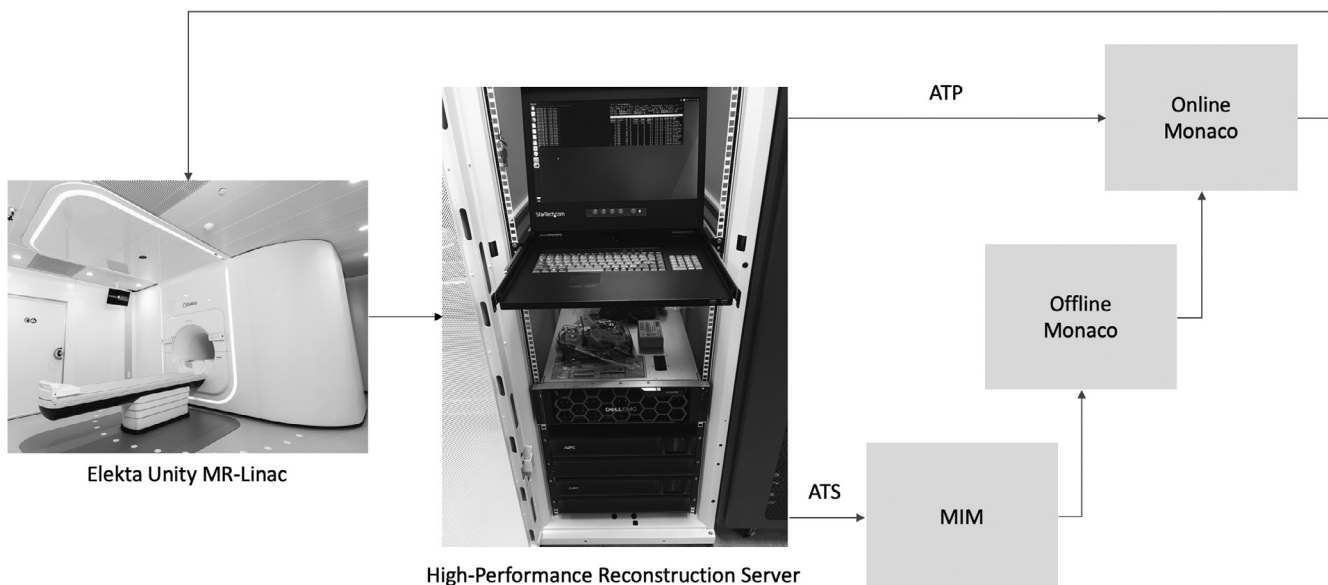

Elekta Unity MR-Linac

High-Performance Reconstruction Server

Fig. 2. System architecture employed to reconstruct 4D-MRI data for MR-guided online adaptive abdominal SBRT. A high-performance reconstruction server was positioned on the local machine network of the Elekta Unity MR-Linac. Raw k-Space data was transferred to the server. Reconstructed DICOM images were transferred to MIM or Monaco depending on use of Adapt-To-Position (ATP) or Adapt-To-Shape (ATS) workflows. The daily adaptive plans were then delivered on the MR-Linac (see text for details).

2.3.2. ATP workflow

For ATP patients, the daily pre-beam MotAvg or MidP images were rigidly registered with local alignment of the GTV or CTV in Monaco using either the planning CT or prior fraction MR as reference images. Of the four available adaptive planning methods for ATP in Monaco, adaptive plans were generated by optimizing both shapes and weights from segments [4,14]. In this approach, reoptimization is performed using warm start optimization to reproduce the reference plan dose [15]. The optimization is performed using the reference images and structures, but with a shifted isocenter based on the rigid registration of daily and reference images.

2.3.3. ATS Workflow: contour editing

Two strategies were employed to reduce contour editing time when the ATS workflow was utilized for daily adaptation. First, OARs were only verified within a 2 cm expansion around the PTV (i.e., OAR editing was limited to the high dose regions of the plan). The second strategy was to utilize a parallel workflow for contour

editing (see Fig. 3). Briefly, the structure set from the planning CT (or one of the prior fraction MR images) was transferred to the daily MR. The structure set was then split into three sub-structure sets: i) targets and proximal OARs within the 2 cm edit ring, verified by radiation oncologists, ii) non-deforming OARs in the IMRT constraints of the plan (e.g., kidneys, liver, spinal cord), verified by radiation therapists, and iii) structures that affect dose calculation (e.g., external patient, bone, air, lungs, and implants (e.g., stents, clips, calcifications), verified by physicists. The team members then edited contours simultaneously on three networked MIM workstations. After editing, the structures were concatenated into a single structure set, reviewed and approved by the radiation oncologist, and then transferred to Monaco for adaptive plan generation. A similar approach was recently reported [16].

2.3.4. ATS Workflow: replanning

Monaco supports six adaptive planning methods for ATS [4]. Adaptive plans were generated using the optimize weights and

Fig. 3. Parallel contouring workflow used for Adapt-To-Shape (ATS) MR-guided online adaptive abdominal SBRT. Contours were transferred from the reference studyset (e.g., planning CT or prior fraction MR) to daily MR. The transferred structure set was then split into physician (targets and organs at risk within 2 cm edit ring of PTV), therapist (non-deforming organs at risk in IMRT constraints), and physicist (patient model) sub-structure sets. Contour touchup was performed in parallel using three networked MIM workstations. Approved contours were then concatenated into one structure set and transferred to Monaco for adaptive plan generation, review, and approval.

shapes from fluence method. This method effectively performs a full re-plan using the updated structure set reflecting the anatomy at the time of the daily pre-beam 4D acquisition. Bulk density over-rides of patient, bone, air, lungs, and any implants were verified prior to reoptimization. Unlike the reference plan, multi-criteria optimization was not performed during the initial fluence calculation for the adaptive plan. However, analogous to the reference plan, Pareto optimization was utilized for segment optimization. In addition, dynamic adjustment of OAR isoconstraints was performed (if necessary) during segment optimization in attempt to improve plan quality.

2.3.5. ATS Workflow: verification imaging

An additional verification 4D-MRI was acquired during plan reoptimization. Prior to beam-on, verification MotAvg or MidP images were loaded into Monaco and registered to the pre-beam MotAvg or MidP images using iso-to-iso alignment. The verification image was used to determine whether significant anatomical changes occurred during recontouring and reoptimization (e.g, targets moving away from original position due to filling or drifts). If variations were deemed significant by the treating physician the verification image was rigidly re-registered to the pre-beam MotAvg or MidP images. Afterwards, an ATP plan was generated on top of the daily ATS plan based on positional isocenter shifts determined from the rigid registration.

2.3.6. Quantitative MR imaging

Quantitative MR imaging (qMRI) for treatment response monitoring was performed simultaneously during plan adaptation in both ATP and ATS workflows (see Fig. 1). Free-breathing intravoxel incoherent motion (IVIM) images were acquired using a diffusion-weighted, fat-suppressed, single-shot, spin echo, echo-planar imaging sequence (TE: 70 ms, TR: 5550 ms, 3 mm in-plane resolution, 30 5 mm slices, acceleration factor = 2.5, b-values: 0, 30, 150, 550 s/mm^2). Although B0 homogeneity varies minimally with gantry rotation [17], for consistency the gantry was positioned at 0 degrees prior to acquisition. Voxelwise true diffusion component (Dt) and perfusion fraction (f) estimates were obtained using the one-parameter approach [18,19]. Quantitative T_2 mapping was performed using an accelerated Carr Purcell Meiboom Gill (CPMG)

sequence with 16 echoes (TE: 16 + n*13 ms, TR: 2500 ms, 2 mm in-plane resolution, 30 5 mm slices, acceleration factor = 2.5). Depending on the degree of respiratory displacement and consistency of breathing, CPMG images were acquired either free-breathing or with navigator-based respiratory triggering at end expiration. Voxelwise T_2 estimates were obtained from mono-exponential fitting of decay curves using nonlinear least squares. All qMRI post-processing used custom Java and Matlab extensions implemented on a dedicated 24 core Intel Xenon 2.4 GHz, 32 GB RAM MIM processing server positioned on the local MR-Linac machine network.

2.3.7. Adaptive plan quality assurance

After review of the adaptive plan and verification images by the radiation oncologist, a secondary dose calculation utilizing a modified Clarkson algorithm with correction for transverse magnetic field was performed [20]. A 3D gamma score >90% using 4 mm/4% criteria was considered in agreement with the daily adaptive plan dose calculated in Monaco. The integrity of the plan transfer from Monaco to the Mosaiq record and verify system was then verified [20]. Finally, monitor units for each beam were verbally verified between Monaco and Mosaiq prior to beam-on.

2.3.8. Beam-on imaging

Beam-on cine imaging was performed at 5 frames per second using a balanced turbo field echo (bTFE) sequence (1.2 mm in-plane resolution (reconstructed), 5 mm slices, TE: 1.9 ms, TR: 3.8 ms, flip angle: 40 degrees). One, two, or three orthogonal planes were prescribed for motion monitoring depending on PTV size. For PTVs less than 2 cm diameter, one cine image plane was prescribed to avoid partial saturation bands from obscuring visualization of the target during treatment delivery.

2.3.9. Post-beam imaging

A post-beam 4D-MRI was acquired immediately following treatment delivery for use in offline dose reconstruction. For ATP patients, dose was reconstructed on the daily pre-beam and post-beam MotAvg or MidP images and compared against the reference plan dose. For ATS patients, dose was reconstructed on verification and post-beam images (following contour propagation from pre-

beam images with manual contour editing if required) and compared against the daily adaptive plan dose. For a subset of patients, the planned (ATS) or reconstructed (ATP) doses were accumulated onto the first fraction MR in MIM. This process employed a conservative approach for OAR evaluation in which the 0.5 cc maximum OAR doses from each fraction were tabulated and summed.

2.4. Post-treatment workflow

Immediately following treatment, the treatment record parameters including MLC and jaw positions per segment, MU per segment, total beam MU, gantry position, were compared against the adaptive plan parameters using tolerances of 1 mm, 0.1 MU, and 0.1 degree, respectively [20]. In addition, the daily adaptive ATP or ATS plan was delivered to an MR-compatible ArcCheck dosimeter (Sun Nuclear, Melbourne, Florida). A 3D gamma score >95% using 3%/3mm criteria was considered to agree with the daily adaptive plan.

3. Results

3.1. Online 4D-MRI

The 4D-MRI acquisition time ranged from 3 to 3.5 min, depending on contrast mode selected by the physician. Raw data transfer times from the MRI host computer to reconstruction server took less than 10 s. Reconstruction times for the MotAvg, MidP, and respiratory binned images were 2, 3.7, and 6.4 min, respectively. Although the MidP image is derived from the binned 4D images, due to computation times required to perform 3D gradient nonlinearity correction on each respiratory phase and write DICOM images for each respiratory phase, the output of the images was reversed and the MidP images were written to disk before the binned 4D phase images. This approach permitted the ATP or ATS workflow to start in the shortest time possible while still pro-

viding the individual binned 4D images for motion assessment. As shown in Supplementary Table S1, MidP images were selected for use in two of the eleven patients, due to larger respiratory motion. Three additional patients also demonstrated larger respiratory motions (>0.8 cm), however, MotAvg images were selected due to inconsistent breathing of these patients. MotAvg images were selected for the remaining patients with smaller respiratory motion. The respiratory binned images were used for each patient to verify the ITV.

Fig. 4 displays representative MotAvg, MidP, and respiratory binned 4D-MR images for a liver patient with significant respiratory motion (>2 cm). Although the radial trajectory from 3D Vane is effective at minimizing in-plane motion artifacts (i.e., in the axial MotAvg images), large respiratory-induced displacements can result in blurring along the superior-inferior direction. The blurring can obscure delineation of small targets and OAR boundaries (see arrows) and may contribute to registration uncertainties in the ATP workflow. Although the MotAvg image was fastest to reconstruct, the MidP images demonstrate reduced blurring and sharp target and OAR boundaries in the presence of large respiratory induced displacements and were used for this patient.

3.2. Adaptive workflow

As shown in Supplementary Table S1, 50% of the treatments utilized the ATS workflow; the remaining treatments utilized the ATP workflow. Fig. 5 displays images of a liver SBRT patient treated on the Unity (full color version in Supplementary Fig. S1). Dysfunctional hepatocytes, secondary to irradiation, are visible on the 1-month follow up diagnostic image, and correlate with the accumulated dose. None of the ATS patients in this work required subsequent ATP based on evaluation of the verification images prior to delivery of the adaptive plan. For one ATS patient, the 0.5 cc accumulated maximum dose to OARs was sufficiently below the reference plan dose that an additional treatment fraction was prescribed and delivered.
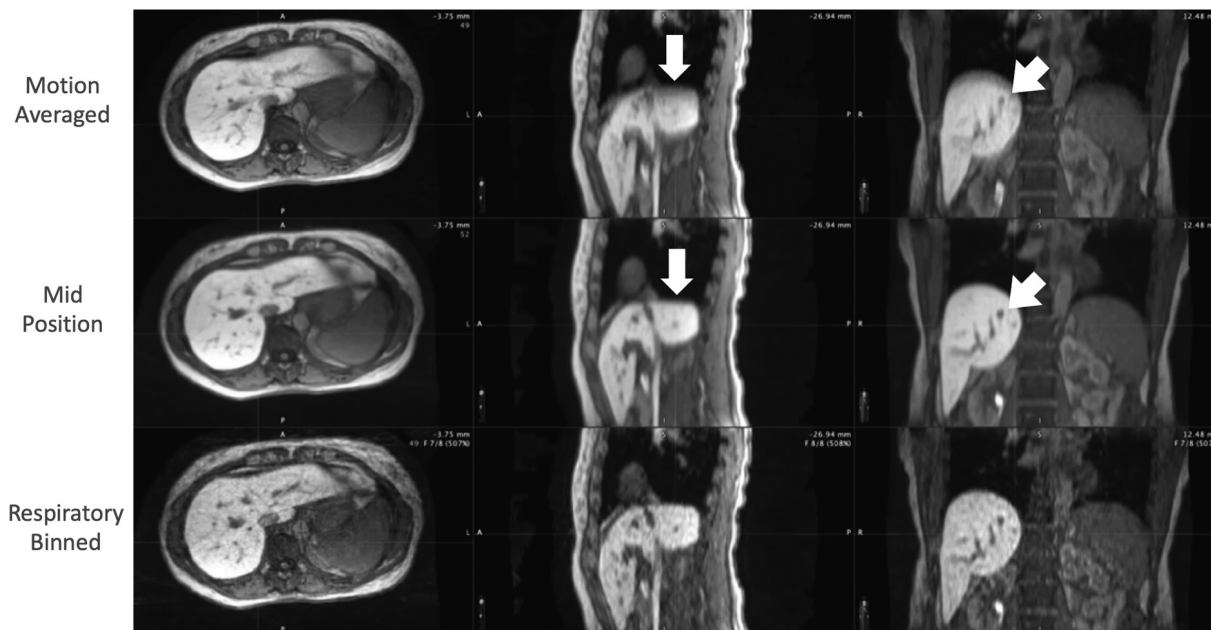

Fig. 4. Reconstructed MR-Linac 4D-MR images for representative liver patient with significant respiratory induced displacement (>2cm). Motion averaged images (top row) have the shortest time-to-image, but can exhibit blurring that may obscure target and OAR boundaries and introduce errors during co-registration. Mid-Position images (middle row) take longer to reconstruct but demonstrate sharp boundaries even in the presence of large respiratory displacements. One phase from respiratory binned images (bottom row) shown for reference image quality.
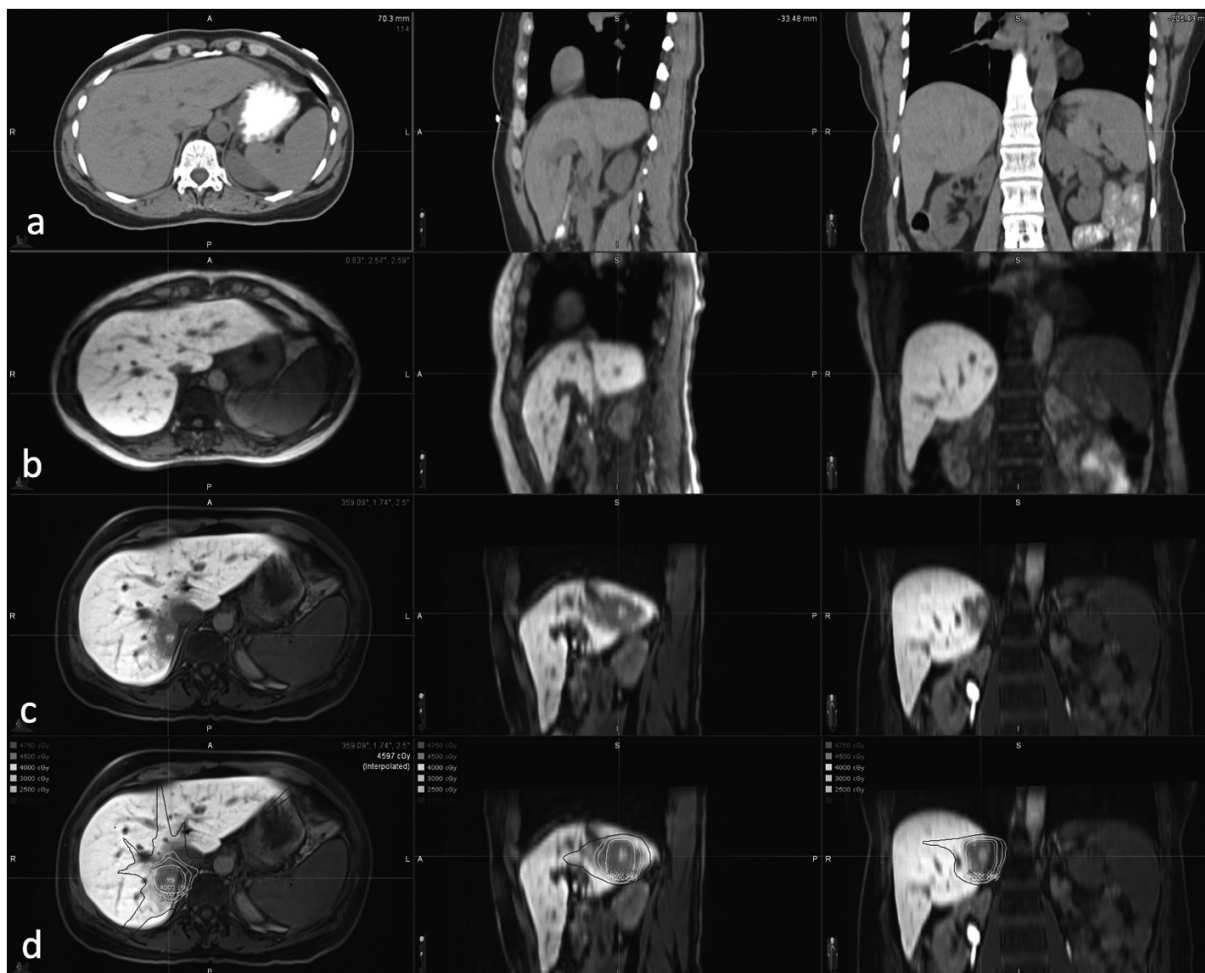
Fig. 5. Liver patient treated with MR-guided online adaptive abdominal SBRT on an Elekta Unity MR-Linac (same patient as Fig. 4). The small liver lesion is not visible on mid-position CT (a), but is visible on breath-hold post-Eovist T1 MR sim images (b). The one month follow up diagnostic breath-hold post-Eovist T1 MR (c) demonstrates reduced Eovist uptake secondary to hepatocyte damage from radiotherapy, evident when the accumulated dose from all three SBRT fractions is overlaid (d).

3.3. Quality assurance

The mean pre-treatment ArcCheck 3D Gamma passing rate was 99.4% (97.8–100.0%) for all patient reference plans. The mean post-treatment ArcCheck 3D Gamma passing rate was 99.3% (96.2–100.0%) for all daily adaptive plans. Supplementary Table S1 displays the ArcCheck 3D Gamma passing rate for each patient in the cohort. The mean 3D Gamma passing rate for adaptive plan secondary dose calculation was 97.5% (92.1–100.0%). The lower passing rates were observed in lateral lesions, due to the modified Clarkson algorithm not incorporating loss of scatter. No deviations between planned and delivered parameters were detected during post-treatment chart checks.

3.4. Quantitative imaging

Respiratory triggered CPMG, quantitative T2 map, free breathing IVIM, and quantitative true diffusion (Dt) map for a representative pancreas adenocarcinoma patient are shown in Supplementary Fig. S2.

3.5. Overall treatment times

The median overall treatment time for abdominal SBRT was 46 min using the ATP workflow and 62 min using the ATS work-flow. The breakdowns of treatment times for each major task of ATP and ATS workflows are shown in Supplementary Fig. S3.

4. Discussion

We have implemented a 4D-MRI driven MRgOART process for free-breathing abdominal SBRT on a 1.5 T Elekta Unity MR-Linac. Our process was successfully used to treat eleven patients with abdominal malignancies. Both ATP and ATS approaches were utilized for clinical treatments. For ATS, a parallel contouring workflow was employed. With our MRgOART workflow shown in Fig. 1, the MRI is continuously acquiring data the entire time the patient is on the treatment table. The non-commercial aspects of our approach include the use of 4D-MRI, parallel contouring for ATS, and our secondary dose calculation software for adaptive plan quality assurance.

The 3D GAR SoS method was utilized for respiratory-correlated 4D-MRI in this work. The decision to use this method was based on prior work in which it was shown that high quality 4D-MR images with 1–2 mm accuracy could be generated from the 3D GAR SoS method within five minutes [9], which we reasoned to be clinically acceptable. This benchmark was performed at 3 T with a phased array receive coil density nearly 3 times higher than that available on the Unity system. The receive coil and field strength combination permitted a shorter 4D-MRI acquisition in the benchmark

study. With the lower receive coil density and field strength on the Unity system (1.5 T with 8 receive channels) a longer acquisition time (higher spoke density) was required to achieve adequate signal-to-noise ratio images. In addition to longer acquisition times, the reconstruction times for MotAvg and MidP images were longer than desired, despite the use of a high-performance reconstruction server to parallelize the reconstruction [9]. This was due, in part, to portions of the reconstruction code being performed in Matlab. Faster implementations are under development.

In this work, an ITV approach based on 4D-CT or 4D-MR images of patients was employed for motion management in free-breathing abdominal SBRT. Future work will utilize MidP PTV margins derived from the daily 4D-MRI. It has been shown that irradiated volumes can be significantly reduced using the MidP approach compared to ITV approaches [21].

The use of free-breathing treatments for abdominal SBRT may be considered suboptimal. However, free-breathing treatments maximize the delivery duty cycle, thereby minimizing potential deviations between planned and actual anatomy during delivery. Although breath-hold gating deliveries may result in smaller margins, the efficacy of the approach is dependent on the ability of patients to perform consistent breath-holds during treatment. In addition, by reducing the delivery duty cycle, gating extends the delivery time in an already time-consuming online adaptive process. Trailing [22], tracking [23], or real-time plan adaptation [24] may be more desirable options. As an initial step toward trailing, the Unity system does support an ATS followed by ATP approach, which enables correction of positional shifts due to filling or drifts during ATS while the patient is on the table. Although none of the ATS patients in this cohort required subsequent ATP based on verification images, we have treated other disease sites (e.g., prostate SBRT) that have benefited from this approach.

Navigator-based respiratory triggered acquisitions to minimize motion artifacts are supported on the Unity system. However, because only free-breathing treatment *deliveries* are currently supported, acquisition of triggered images at end-inspiration or end-expiration would result in a systematic offset between planned and delivered anatomies. This was a major factor influencing the decision to implement 4D-MRI for abdominal SBRT on the Unity.

The parallel contouring workflow utilized all available human resources of the Unity team during ATS treatments. It was previously shown that such a parallel process can reduce contour editing time by more than 50% [16]. A potentially even greater advantage is that the parallel workflow provides time for each team member to concentrate on his/her individual tasks. Anecdotally, this reduced the pressure felt by team members holding up the adaptive planning process. In turn, this reduced pressure may translate into a reduced potential for error.

Monaco supports four online adaptive planning methods for ATP and six online adaptive methods for ATS. During preliminary testing, we found that the optimize shapes and weights from segments approach was the only ATP adaptation method capable of reproducing goal doses, even in the presence of small shifts (<5mm). Similar results were recently reported [4]. For ATS, the use of Pareto optimization limited OAR constraint weights to 10.0 during segment optimization, effectively tilting the optimizer toward targets. This was performed with the theory that limiting the OAR constraint weights would speed up reoptimization in the online workflow. A comprehensive comparison of constrained versus Pareto optimization times remains to be performed.

Due to software limitations, an offline Monaco system was used for adaptive plan generation in the ATS workflow, leaving an online Monaco system sitting idle. An alternative approach would be to plan (as well as contour) in parallel, generating a pseudo-ATS plan on the daily MR simultaneously while recontouring is being performed. This would enable comparison between warm start and full fluence reoptimized plans, with the potential of saving time by skipping full fluence reoptimization if the warm start plan is sufficient for the anatomy of the day. This alternative approach will be one focus of future investigations.

In this work, MotAvg or MidP images derived from a pre-beam respiratory-correlated 4D-MRI were used for adaptive plan generation, with one, two, or three plane 2D cine images used for real-time motion monitoring during treatment delivery. Ideally, prospective, dynamic volumetric imaging would be utilized throughout a treatment fraction, facilitating continuous 3D monitoring of anatomy, dynamic dose reconstruction throughout treatment, and potentially real-time plan adaptation [24]. However, even with the high-performance reconstruction server employed in this work, current volumetric MRI acquisition and reconstruction times prohibit volumetric imaging at the spatiotemporal resolutions required for radiotherapy. Recent advances in deep learning based MRI reconstructions [25,26] may enable real-time volumetric imaging.

It has been suggested that specific absorption rate (SAR) limits could be an issue for real-time motion monitoring at 1.5 T when balanced steady-state free-precession sequences are used for cine imaging (analogous to the sequences used in this work). However, SAR limits were never exceeded for any of the patients treated on the Unity. Furthermore, the higher field strength of the Unity system presents opportunities to utilize other sequences for motion monitoring to obtain contrasts more appropriate for different disease sites. This will be one focus of future work.

Finally, the system architecture of including a high-performance compute device on the local MR-Linac machine network facilitates additional utility beyond 4D-MRI reconstruction. Other advanced MRI techniques (e.g., MR fingerprinting) also rely on computationally demanding reconstruction algorithms and may become clinically feasible in an online environment with this architecture.

Acknowledgements

Appendix A. Supplementary data

Supplementary data to this article can be found online at https://doi.org/10.1016/j.ctro.2020.05.002.

References

[1] Reyngold M, Parikh P, Crane CH. Ablative radiation therapy for locally advanced pancreatic cancer: techniques and results. Radiat Oncol 2019;14(1):95.

[2] Lagendijk JJW, Raaymakers BW, van Vulpen M. The magnetic resonance imaging-Linac system. Semin Radiat Oncol 2014;24(3):207–9.

[3] Kooreman ES et al. Feasibility and accuracy of quantitative imaging on a 1.5 T MR-linear accelerator. Radiother Oncol 2019;133:156–62.

[4] Winkel D et al. Adaptive radiotherapy: The Elekta Unity MR-linac concept. Clin Transl Radiat Oncol 2019:1–6.

[5] Stemkens B, Paulson ES, Tijssen RHN. Nuts and bolts of 4D-MRI for radiotherapy. Phys Med Biol 2018;63(21). Ahead of print.

[6] Wolthaus JWH, Sonke JJ, Van Herk M, Damen EMF. Reconstruction of a time-averaged midposition CT scan for radiotherapy planning of lung cancer patients using deformable registrationa. Med Phys 2008;35(9):3998–4011.

[7] Paulson ES, Erickson B, Schultz C, Allen Li X. Comprehensive MRI simulation methodology using a dedicated MRI scanner in radiation oncology for external beam radiation treatment planning. Med Phys 2015;42(1):28–39.

[8] Feng L, Axel L, Chandarana H, Block KT, Sodickson DK, Otazo R. XD-GRASP: Golden-angle radial MRI with reconstruction of extra motion-state dimensions using compressed sensing. Magn Reson Med 2015:1–14.

[9] Mickevicius NJ, Paulson ES. Investigation of undersampling and reconstruction algorithm dependence on respiratory correlated 4D-MRI for online MR-guided radiation therapy. Phys Med Biol 2017;62(8):2910–21.

[10] Hissoiny S, Ozell B, Bouchard H, Despŕs P. GPUMCD: a new GPU-oriented Monte Carlo dose calculation platform. Med Phys 2011;38(2):754–64.

[11] Hissoiny S, Raaijmakers AJE, Ozell B, Després P, Raaymakers BW. Fast dose calculation in magnetic fields with <tt>GPUMCD</tt>. Phys Med Biol 2011;56(16):5119–29.

[12] Chen X, Paulson ES, Ahunbay E, Sanli A, Klawikowski S, Li XA. Measurement validation of treatment planning for a MR-Linac. J Appl Clin Med Phys 2019:28–38.

[13] Boesiger P, Pruessmann KP, Weiger M, Bornert P. Advances in sensitivity encoding with arbitrary k-space trajectories. Magn Reson Med 2001;46(4):638–51.

[14] Ahunbay EE et al. An on-line replanning scheme for interfractional variations. Med Phys 2008;35(8):3607–15.

[15] Ahunbay EE, Ates O, Li XA. An online replanning method using warm start optimization and aperture morphing for flattening-filter-free beams. Med Phys 2016;43(8):4575–84.

[16] Zhang J, Ahunbay E, Li XA. Technical Note: Acceleration of online adaptive replanning with automation and parallel operations. Med Phys 2018;45(10):4370–6.

[17] Tijssen RHN et al. MRI commissioning of 1.5T MR-linac systems – a multi-institutional study. Radiother Oncol 2019;132:114–20.

[18] Meeus EM, Novak J, Withey SB, Zarinabad N, Dehghani H, Peet AC. Evaluation of intravoxel incoherent motion fitting methods in low-perfused tissue. J Magn Reson Imaging 2017;45(5):1325–34.

[19] Barbieri S, Donati OF, Froehlich JM, Thoeny HC. Impact of the calculation algorithm on biexponential fitting of diffusion-weighted MRI in upper abdominal organs. Magn Reson Med 2016;75(5):2175–84.

[20] Chen GP, Ahunbay E, Li XA. Technical Note: Development and performance of a software tool for quality assurance of online replanning with a conventional Linac or MR-Linac. Med Phys 2016;43(4):1713–9.

[21] Wolthaus JWH et al. Comparison of different strategies to use four-dimensional computed tomography in treatment planning for lung cancer patients. Int J Radiat Oncol Biol Phys 2008;70(4):1229–38.

[22] Trofimov A, Vrancic C, Chan TCY, Sharp GC, Bortfeld T. Tumor trailing strategy for intensity-modulated radiation therapy of moving targets. Med Phys 2008;35(5):1718–33.

[23] Keall PJ, Kini VR, Vedam S, Mohan R. Motion adaptive X-ray therapy: a feasibility study. Phys Med Biol 2001;46:1–10.

[24] Kontaxis C et al. Towards fast online intrafraction replanning for free-breathing stereotactic body radiation therapy with the MR-linac. Phys Med Biol 2017;62(18):7233–48.

[25] Hammernik K et al. Learning a variational network for reconstruction of accelerated MRI data. Magn Reson Med 2018;79(6):3055–71.

[26] Qin C, Schlemper J, Caballero J, Price A, Hajnal JV, Rueckert D, Convolutional recurrent neural networks for dynamic MR image reconstruction, 2017, 1–9.